Resonant Thickening of Disks by Small Satellite Galaxies

J. A. Sellwood
Department of Physics and Astronomy, Rutgers, The State University of New Jersey, 136 Frelinghuysen Road, Piscataway, NJ 08854-8019
Isaac Newton Institute, University of Cambridge, 20 Clarkson Road, Cambridge CB3 0EF, England
sellwood@physics.rutgers.edu

Robert W. Nelson
Theoretical Astrophysics 130-33, California Institute of Technology, Pasadena CA 91125
nelson@tapir.caltech.edu

and

Scott Tremaine
Canadian Institute for Theoretical Astrophysics, University of Toronto, 60 St George Street, Toronto M5S 3H8, Canada
Department of Astrophysical Sciences, Peyton Hall, Princeton University, Princeton, NJ 08544-1001
tremaine@astro.princeton.edu

ABSTRACT

We study the vertical heating and thickening of galaxy disks due to accretion of small satellites. Our simulations are restricted to axial symmetry, which largely eliminates numerical evolution of the target galaxy but requires the trajectory of the satellite to be along the symmetry axis of the target. We find that direct heating of disk stars by the satellite is not important because the satellite's gravitational perturbation has little power at frequencies resonant with the vertical stellar orbits. The satellite does little damage to the disk until its decaying orbit resonantly excites large-scale disk bending waves. Bending waves can damp through dynamical friction from the halo or internal wave-particle resonances; we find that wave-particle resonances dominate the damping. The principal vertical heating mechanism is therefore dissipation of bending waves at resonances with stellar orbits in the disk. Energy can thus be deposited some distance from the point of impact of the satellite. The net heating from a tightly bound satellite can be substantial, but satellites that are tidally disrupted before they are able to excite bending waves do not thicken the disk.

Subject headings: galaxies: evolution — galaxies: kinematics and dynamics — galaxies: internal structure — galaxies: interactions — galaxies: formation

1. Introduction

Disk galaxies are observed to be cold and thin, with typical scale heights only 10% of their radial scale lengths. The accretion of satellite galaxies should strongly heat and thicken disks, so this observation limits the satellite infall rate. Tóth & Ostriker (1992; hereafter TO) pointed out that thin galactic disks may therefore set important cosmological constraints.

TO estimate the energy deposited in the disk during an accretion event in a simplified manner. They assume that the satellite galaxy spirals into the parent galaxy on a near-circular orbit as it loses energy through dynamical friction to both the dark matter halo and the disk. They determine the rate of energy loss to both components using Chandrasekhar's dynamical friction formula (Binney & Tremaine 1987, §7.1), and deposit the energy locally in the halo and disk, sharing the disk energy between vertical and horizontal motions in a fixed ratio. TO recognize that their treatment omits all collective effects in the response, but argue that had they "treated the problem as one of exciting modes in the disk...[they] would have found the same overall energy change in the disk."

It is not obvious that this claim is correct; there are good reasons to believe that in-plane heating will be increased while vertical heating could be *reduced* by collective effects. A swing-amplified spiral response (see Binney & Tremaine 1987 for a review) will always extract energy from the potential well of the target galaxy, thereby adding to the energy deposited into in-plane random motion. On the other hand, the following simple thought experiment suggests that vertical heating could be small. Let us imagine that the disk is very stiff so that the eigenfrequencies of its collective bending modes are very high. In this case, the time-dependent perturbation of a passing satellite will not contain power at frequencies which are resonant with any collective modes, and there is little internal heating; the disk acts like a rigid plate and the only effect of interaction with the satellite is to tilt or translate the disk. We will develop these ideas further for more realistic disks in §2.

Many of TO's simplifying approximations are avoided in fully self-consistent N-body simulations, which have been widely used to study the merger of small satellites with a large disk galaxy (Quinn & Goodman 1986; Pfenniger 1991; Quinn, Hernquist & Fullagar 1993; Walker, Mihos & Hernquist 1996; Athanassoula 1996; Huang & Carlberg 1997). These simulations have mostly confirmed that disks are strongly heated by the accretion of a $\sim 10\%$ mass satellite and have elucidated other effects, such as the stripping and tidal disruption of the satellite as it approaches the target galaxy, and the tilting of the disk plane due to the gravitational torque from the satellite. Many of these calculations have begun with models in only approximate equilibrium, and suffered from relaxation and other numerical noise. Numerical relaxation is reduced by particle softening, but excessive softening impairs the ability of the disk to support collective modes. Of these simulations, that of Walker et al. was most successful at suppressing relaxation while maintaining a small softening parameter, but their single simulation did not enable them to reach a firm conclusion on many of the issues raised by TO. Huang & Carlberg argue that TO overstate the disk heating associated with mergers; they find that the disk absorbs some of the orbital angular momentum of the satellite simply by tilting, which reduces the energy of vertical oscillation available to thicken the disk. These simulations have been valuable, but a better appreciation of the physics of the heating process is crucial if we are to understand how to generalize the simulation results.

Since it is the thinness of disks that is hardest to preserve, we focus here on how vertical heating is affected by collective effects, and say little about in-plane heating. Moreover, vertical heating is a cleaner problem than radial heating, since there is no radial redistribution of the disk matter. Vertical heating is largely unaffected by the energy deposited into in-plane motion in the short run; it should be noted however, that molecular clouds can gradually scatter horizontal motion into vertical motion, thereby thickening the disk over timescales comparable to a Hubble time (Carlberg 1987).

We first discuss heuristically, in §2, how energy might be deposited by a satellite into vertical heat in the disk. We test these ideas using numerical simulations which are designed to avoid the complications caused by numerical relaxation and rearrangement of angular momentum. Our simulations utilize an axisymmetric grid and scarcely evolve when unperturbed. They avoid both internal relaxation and softening while also being much faster than the direct N-body methods adopted in previous studies. We are therefore able to quantify the heating and to explore more parameter space. The assumption of axisym-

metry restricts us to mergers that occur along the symmetry axis, however.

There are several mitigating effects (tidal disruption of the satellite, late star formation, infalling cold gas, etc.) that may reduce the thickening caused by satellite mergers. We do not address these issues here, but focus on the detailed physical process of vertical heating by a rigid massive satellite.

2. A heuristic discussion of disk heating

Chandrasekhar's dynamical friction formula assumes that the disk and halo stars are free particles that travel on isotropically distributed, straight-line orbits, and neglects the self-gravity of the response to the perturbing satellite. Any heating calculation based on that formula thus ignores both the periodic orbital structure of the disk stars, and the possibility of exciting large-scale collective modes in the form of bending and density waves. We shall examine each of these effects in isolation, even though they are closely related.

2.1. Direct heating

We first consider an idealized problem that isolates the effects of the periodic orbital structure of the disk stars. Stars near the disk mid-plane oscillate vertically with a frequency $\kappa_z^2 = \frac{1}{2}\partial^2\Phi/\partial z^2$, where $\Phi(\mathbf{x})$ is the gravitational potential. The tidal field from the passing satellite can be considered to accelerate the star relative to the disk mid-plane. For a satellite of mass M_s moving at relative speed v and impact parameter b, one finds the mean change in the vertical energy per unit mass of a disk star during a single satellite passage with random orientation is (Spitzer 1958)

$$\Delta E_z = \frac{h^2}{3}\left(\frac{GM_s}{b^3\kappa_z}\right)^2 \beta^2 L(\beta), \qquad (1)$$

where h is the rms thickness of the disk and the parameter $\beta = 2\kappa_z b/v$ is of order the characteristic passage time of the satellite divided by the orbital period of the star. The dimensionless function $L(\beta)$ is unity for $\beta \to 0$ and exponentially small for $\beta \gg 1$. Figure 1 shows that the net energy transfer peaks at $\beta \sim 1$, when the forcing contains significant power near κ_z and thus is resonant with the stellar orbit. At high velocities ($1/\beta \gg 1$), the net energy transferred is nearly the same as for a free particle, and thus varies as β^2 or v^{-2}. At low velocities ($1/\beta \ll 1$),

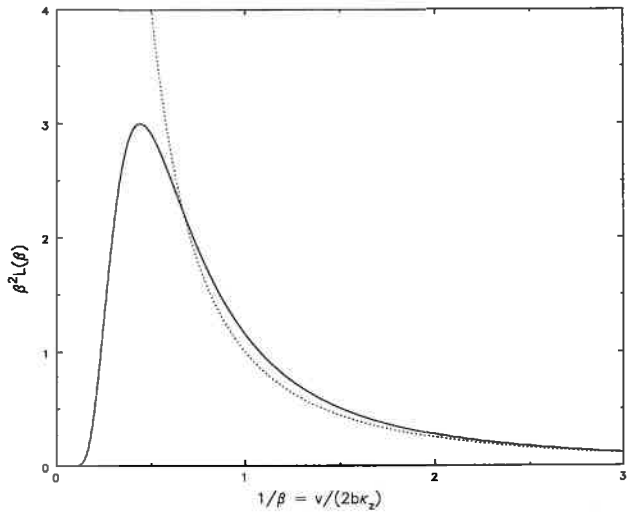

Fig. 1.— The dimensionless factor in the mean energy transferred to a harmonically bound star (solid line) due to the tidal force of a passing satellite (from equation 1). For high velocities, the energy transfer is the same as for a free particle (dotted line), but the transfer is exponentially small at low velocities when the star responds adiabatically.

however, the star responds adiabatically and reversibly so the energy transfer is exponentially small. In other words, only stars with impact parameters $b \lesssim v/\kappa_z$ gain energy from a satellite passage. TO's free-particle approximation effectively sets $\kappa_z \to 0$ so that all stars gain energy.

The h^2 dependence in equation (1) indicates that the heating is tidal. Direct heating vanishes as the disk becomes razor thin, both because $h \to 0$ and also because $\kappa_z \to \infty$.

2.2. Bending waves in razor-thin disks

A self-gravitating disk supports collective modes, such as bending waves. The simplest approximate analysis was given by Toomre (1966), who derived a dispersion relation for bending waves in an idealized razor-thin membrane with uniform surface density Σ and horizontal velocity dispersion σ; the self-gravity of the sheet resists vertical distortions in much the same way as elasticity in conventional membranes. Toomre's dispersion relation reads

$$\omega^2 = \nu_h^2 + 2\pi G\Sigma|k| - \mathbf{k^2}\sigma^2, \qquad (2)$$

where k is the horizontal wavenumber, and we have added a contribution $\nu_h^2 = \frac{1}{2}\partial^2\Phi_h/\partial z^2$ from the ver-

tical frequency of free oscillations due to a halo potential $\Phi_{\rm h}$. This dispersion relation says that the disk becomes unstable for sufficiently large k, but in practice the instability is usually suppressed by nonzero disk thickness. Once excited, such waves propagate with group velocity

$$c_{\rm g} = \frac{d\omega}{dk} = {\rm sgn}(k)\frac{\pi G\Sigma}{\omega}\left(1 - \frac{2k}{k_{\rm J}}\right), \qquad (3)$$

where $k_{\rm J} = 2\pi G\Sigma/\sigma^2$.

Equation (2) suggests that long-wavelength modes have eigenfrequencies $\omega \gtrsim \nu_{\rm h}$. The exception is the $m = 1$ tilt mode (Sparke & Casertano 1988), which would be neutral in a spherical halo. The gravitational field of the satellite excites bending waves if and only if the Fourier transform of the external perturbation has power at the mode frequencies.

What happens to energy deposited in Toomre's membrane in the form of bending waves? The wave cannot damp internally; it loses energy only by dynamical friction with the halo (Dubinski & Kuijken 1995, Nelson & Tremaine 1996). Since direct heating is also negligible (§2.1), a uniform membrane would not be heated at all by a satellite passage.

The modes of cold, disk-like membranes were investigated by Hunter & Toomre (1969). Waves in a cold, axisymmetric disk may propagate all the way to the disk edge. Thus they found a spectrum of disk modes containing both discrete and continuous eigenfrequencies, depending on the sharpness of the disk edge. In a membrane with non-zero horizontal velocity dispersion, waves that would otherwise reach the disk edge may encounter a turning point where $c_{\rm g} = 0$ ($k = k_{\rm J}/2$ in equation (3)) and can be trapped to form a discrete mode (Sellwood 1996).

What happens to the energy deposited in such systems by bending waves? Once again, discrete modes damp only by dynamical friction with the halo, and thus do not heat the disk. Continuous modes can also damp by nonlinear effects that may become important if the mode propagates to the disk edge (Hunter & Toomre 1969); however, in this case only the edge of the disk is heated.

In summary, a satellite passage does not heat razor-thin disks at all, except possibly at their outer edge.

2.3. Bending waves in realistic disks

Razor-thin disks are unrealistic because all of the stars are forced to move together in the vertical direction. In real disks, stars oscillate vertically at finite frequencies, allowing bending waves to damp through wave-particle interactions (Landau damping). The simplest model that includes this effect is a planar distribution of stars which is infinite and homogeneous in the x- and y-directions and held together by self-gravity in the z or vertical direction, with a velocity-dispersion tensor that is independent of position. The phase-space distribution function is (Spitzer 1942, Camm 1950)

$$F(z,{\bf v}) = \frac{\rho_0}{(2\pi)^{3/2}\sigma^2\sigma_z}\exp\left(-\frac{v_x^2+v_y^2}{2\sigma^2} - \frac{E_z}{\sigma_z^2}\right), \quad (4)$$

where the vertical energy $E_z = \frac{1}{2}v_z^2 + \Phi(z)$, ρ_0 is the mid-plane density, and σ and σ_z are constants equal to the velocity dispersions in any horizontal direction and in z. The rms thickness for a Spitzer sheet $h \simeq 0.365\sigma_z/(G\rho_0)^{1/2}$.

A mathematical description of wave propagation in the Spitzer sheet requires a solution of the linearized Boltzmann and Poisson equations for the dispersion relation $\omega(k)$ (Toomre 1966, 1983, 1995; Araki 1985; Weinberg 1991). The result is not analytic and surprisingly more complicated than equation (2). There are no real eigenfrequencies; all waves are Landau damped. Stars whose natural vertical oscillation frequency $\kappa_z(E_z)$ resonates with the apparent (Doppler-shifted) frequency $\omega - kv$ of the bending wave can absorb energy from the wave, converting wave energy into random motion in the sheet. In general, short-wavelength modes $kh \gtrsim 0.5$ damp in less than one wavelength (Toomre 1983, Weinberg 1991), while long-wavelength modes $kh \ll 1$ can propagate large distances.

The energy deposited in bending waves cannot be calculated accurately without first knowing the shapes and frequencies of the bending eigenmodes of the disk. We expect, however, that the total energy deposited in a large-scale bending mode with eigenfrequency ω during one passage of a satellite is of order

$$\Delta E_w \sim M_d\left(\frac{GM_s}{va}\right)^2 \mathcal{L}(\beta'), \qquad (5)$$

where M_d is the disk mass, a is the scale length of the disk, $\beta' = \omega a/v$, and $\mathcal{L}$ is exponentially small when

$\beta' \gg 1$. The major differences between direct heating (equation 1) and heating by excitation of bending waves are that (i) since the typical modal frequency $\omega \ll \kappa_z$, as the satellite slows the stars respond adiabatically and stop absorbing energy well before the modes; (ii) since direct heating occurs through tidal forces, it is suppressed by a factor $(h/a)^2$.

In disks where surface density and dispersions vary slowly with distance, long-wavelength modes propagate until the wave enters a region where the vertical frequency of the majority of stellar orbits is nearly resonant with the wave frequency, $\omega \simeq \kappa_z(R)$. Significant damping occurs if the Doppler-shifted frequency is within one or two times the 'thermal width' of the resonance,

$$\left|\frac{\mathrm{Re}(\omega) - \kappa_z}{k\sigma}\right| \lesssim 1 \text{ or } 2. \qquad (6)$$

Wave-particle interaction at vertical resonances is the primary mechanism which converts the energy of a long-wavelength bending wave into internal heat and thickens the disk. Vertical resonances may occur at radii far from the position where the wave is initially excited.

Exceptionally, the principal axis of the entire disk/halo can be re-aligned by a satellite approaching off axis (Huang & Carlberg 1997). This new equilibrium can be viewed as the trivial tilt mode with zero frequency, which can be excited without causing significant heating.

2.4. Summary

These considerations suggest the following qualitative description for the deposition of the satellite's orbital energy into vertical motion in the disk:

1. An accreting satellite can deposit energy into the disk via resonant excitation of either individual stellar orbits ("direct heating") or long-wavelength collective modes. Direct heating is the closest analog to the energy transfer to free-particle orbits envisaged by TO. Collective modes include both (vertical) bending waves and (horizontal) density waves, but we ignore the latter in the present discussion because they do not thicken the disk directly.

2. At a given position in the disk, only the high-frequency power $\omega \gtrsim \kappa_z$ in the satellite force contributes to direct heating. Little energy is deposited in high-speed passages because the energy transfer $\propto v^{-2}$ in the impulsive limit. In principle, direct heating is most important when the satellite force is near resonance with the disk stars, but the excitation of bending waves is more important in this regime.

3. Power at intermediate frequencies, $\nu_\mathrm{h} \lesssim \omega < \kappa_z$, can excite long-wavelength bending waves.

4. For low-frequency perturbations, $\omega \lesssim \nu_\mathrm{h}$, the disk responds adiabatically and reversibly. The only exception is that low-frequency perturbations can excite the tilt mode (Huang & Carlberg 1997).

5. Bending waves can damp by at least three mechanisms: (a) linear wave-particle resonances (Landau damping); (b) nonlinear damping; (c) dynamical friction with the halo. Waves in real galaxies can also be damped by other mechanisms, for example by viscosity or shocks in the disk gas. Gas dissipation is generally less effective than other damping mechanisms because the mass in gas is much less than the mass in stars except at the disk edge. Only mechanisms (a) and (b) heat the disk.

6. In contrast to the disk, the rate of direct heating of the halo can generally be described by Chandrasekhar's formula. The reason is that the halo contains a rich spectrum of orbital resonances with a wide range of frequencies (Lin & Tremaine 1983; Weinberg 1986).

3. N-body model

We use N-body simulations to assess the importance of collective bending waves. We simulate the interaction between a freely moving, but internally rigid, satellite and an equilibrium disk-halo galaxy model. The satellite orbit lies along the symmetry axis of the galaxy, so the galaxy response can be computed using a two-dimensional axisymmetric grid code described by Sellwood (1996). Since our rigid satellites cannot be tidally stripped or disrupted, they settle intact all the way to the galaxy center; the heating caused in this case is clearly an upper limit. In one separate experiment, we imagine the satellite to dissolve before its orbit has completely decayed.

The disk has an exponential surface-density distribution, contains 30% of the total galaxy mass, M, and is truncated at $R = 5a$, where a is the disk scale length. We give the disk a constant vertical thickness, generally $0.1a$ rms. An exact equilibrium disk model would require a distribution function (DF) that is a function of three integrals, at least one of which is non-classical. Since no such functions are available, we set Toomre's (1964) $Q = 1.5$ to determine the radial velocity dispersion of the disk particles, and estimate orbital velocities using the epicycle approxi-

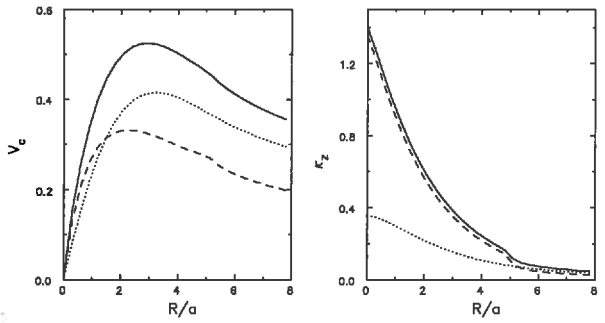

Fig. 2.— (left) The circular velocity and (right) the vertical frequency for small oscillations, as functions of radius. The dashed and dotted curves show the separate contributions of the disk and halo respectively and the full-drawn curves are for the total mass distribution. Thus, κ_z is given by the full-drawn curve on the right while ν_h is given by the dotted curve.

mation and Jeans equations. We also set appropriate vertical velocities to maintain the initial thickness. Such a procedure becomes more approximate as the ratio of the required radial velocity dispersion to the circular velocity rises; this ratio is moderate in our case and the initial model is acceptably close to equilibrium.

The remaining $0.7M$ of the galaxy is in a live and spherical bulge/halo which, however, is not much more extended than the disk. The halo particles are selected from a DF; the procedure for constructing an equilibrium DF in the potential of both the disk and halo will be described in a future paper (Debattista & Sellwood, in preparation). We have opted for a simple isotropic DF of polytropic form

$$f(E) = \begin{cases} (\Phi_* - E)^{n-3/2} & E \le \Phi_* \\ 0, & \text{otherwise} \end{cases} \qquad (7)$$

where n is the polytropic index and Φ_* is the potential at which the halo density is desired to drop to zero. For a polytrope, the density is proportional to the n-th power of the relative potential (Binney & Tremaine 1987, §4.4); we choose $n = 2$. We choose particles from this DF using the procedure described in Sellwood & Valluri (1997).

Overall, the model is close to an exact detailed equilibrium; the worst blemish is a mild imbalance at the outer edge of the disk causing it to spread beyond the initial truncation radius by a few percent. Unperturbed models have been verified to be stable

Table 1. Galaxy Model Parameters

Quantity	Value
Disk	
Model	exponential
Mass M_d	$0.3M$
RMS vertical thickness h	$0.1a$
Toomre Q	1.5
Truncation radius	$5a$
Halo	
Model	$n = 2$ polytrope
Mass M_h	$0.7M$
Truncation radius	$5.62a$
Satellite	
Model	rigid Plummer sphere
Mass M_s	$0.05M$
Core radius r_c	$0.125a$
Numerical Parameters	
Number of disk particles	10^5
Radial grid spacing	$0.1a$
Vertical grid spacing	$0.01a$
Time step	$0.02(a^3/GM)^{1/2}$

and, after some slight adjustment of the disk edge, do not evolve (as will be shown in Figure 6).

Figure 2 shows the rotation curve as well as the radial run of κ_z and ν_h, the frequency of small vertical oscillations in the mid-plane in respectively the total potential and that of the halo only. Our model is somewhat unrealistic for a galaxy since we were forced to choose Φ_* to be the potential at the grid edge, which severely truncates the halo and leads to a falling rotation curve in the outer disk. We justify using it on the grounds that we wish to study physical principles rather than to make detailed comparisons with real galaxies. We also note that the shape of the rotation curve is less important for axisymmetric disturbances of the kind studied here than it is for non-axisymmetric ones.

In most experiments, the satellite is a rigid Plummer sphere having a mass of typically $0.05M$ and a core radius $r_c = 0.125a$. Its motion is computed from the negative of the vector sum of the forces it exerts on all the particles, which are calculated directly and not through the grid. We generally assume that the satellite has fallen from rest at infinity and begin the simulation when it is at a distance of typically $10a$; up to this moment the galaxy is assumed to have re-

sponded to the satellite's approach as a rigid body. In order to prevent large parts of the galaxy from leaving the grid, we shift the grid position at every step by the amount required to keep the center-of-mass of the galaxy centered on the grid. This strategy successfully preserves most particles within the grid; no more than 4% of particles, all from the halo, leave the grid by the end of a freely falling satellite run.

The grid spacing is uniform in both the radial and vertical directions; there are 111 radial nodes spaced at $\delta R = 0.1a$ while the 1125 vertical nodes are spaced with $\delta z = 0.01a$. The vertical structure of the disk is well resolved. We employ 100 000 equal-mass particles and use a time-centered leap-frog integration scheme with $\delta t = 0.02(a^3/GM)^{1/2}$. Energy is conserved to better than 0.1%. The model and numerical parameters are summarized in Table 1.

We have verified that our results are independent of the specific choices for the numerical parameters. We have also obtained similar results using other methods to determine the gravitational field. For checks with fully three-dimensional methods, we substantially suppressed angular momentum transport in the disk by reversing the sense of rotation of half the particles. The disks in these lower-resolution codes thickened a little more, which is to be expected because the vertical cohesion of the disk is diminished when forces are not so well resolved.

All quantities below, and in the Figures, are expressed in units such that $G = M = a = 1$.

4. Disk heating by freely falling satellites

4.1. Numerical results

In our first experiment ("standard run") a satellite of mass $0.05M$ approaches the target galaxy down the symmetry axis on a parabolic orbit. The z-distance of the satellite from the center of mass of the galaxy is shown in figure 3a. Figure 3b shows that the satellite loses energy through dynamical friction in a series of steps, each occurring as it passes through the densest part of the galaxy. Figure 3c shows the time-dependent vertical force as seen by a star at the center of mass of the galaxy. The maximum force during an encounter is $2GM_s/(3^{3/2}r_c^2) = 1.23$ in our units. The initial passages produce a sequence of well-separated impulsive spikes; at late times, as the satellite settles into the disk plane, the spikes become broader and more closely spaced.

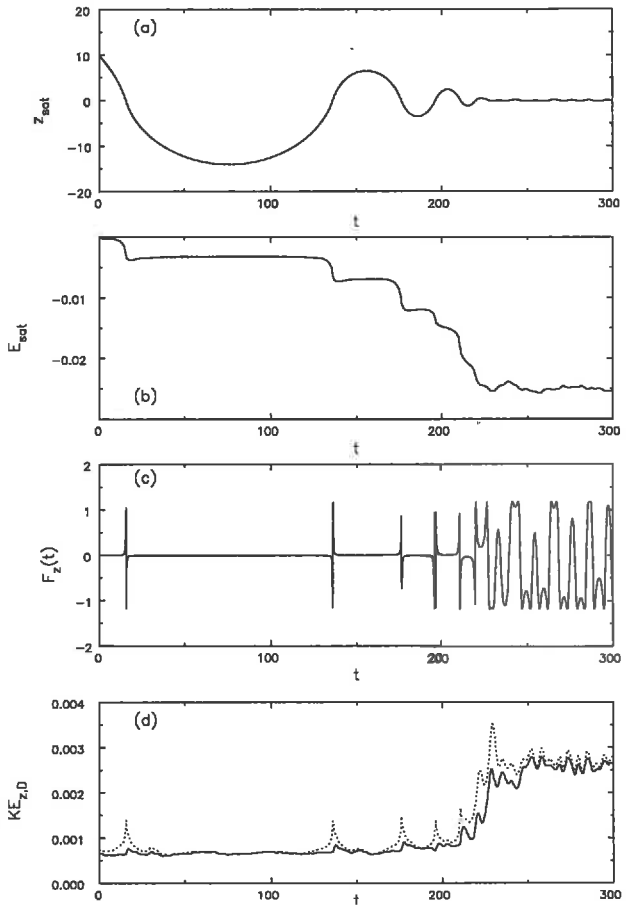

Fig. 3.— The orbital decay in our standard run, in which a 5% satellite falls down the symmetry axis of the target galaxy. (a) The distance between the satellite center and the center of mass of the target galaxy. (b) The kinetic plus potential energy of the satellite, measured in the barycentric frame of the galaxy plus satellite. (c) The vertical acceleration due to the satellite felt by a star at the center of mass of the galaxy. (d) The kinetic energy of vertical motion of the disk particles (dotted) and the kinetic energy of random vertical motion (solid curve).

The vertical heating is shown in Figure 3d. The dotted curve shows the kinetic energy in vertical motion, defined in the frame of the barycenter of the galaxy and satellite. The solid curve shows the kinetic energy of motion relative to the mean velocity of the nearby disk stars. Almost all of the satellite energy is lost to the halo at first and only after the fourth disk passage at $t \simeq 200$ does the disk begin to

heat significantly.

The first passage of the satellite through the disk produces a mild example of a ring formed through the mechanism discussed by Lynds & Toomre (1976). The ring is quite indistinct, however, and the increase in the horizontal random kinetic energy is just a few percent as a result of this first passage. There is little secular increase of the horizontal random motion within the disk until after $t \simeq 200$. In the late stages of the merger, however, the horizontal kinetic energy of random motion doubles.

The substantial vertical heating at late times is associated with violent convulsions of the disk, as shown in Figure 4, after which time the rms disk thickness is some four times its original value. Note that only about 8% of the energy lost by the satellite ends up as increased kinetic energy of vertical motion of the disk particles; the damage caused by this small fraction of the total available energy underscores the extreme fragility of disks.

We have run other experiments starting with both thicker and thinner disks, as well as experiments with other satellite masses. Results from a run with an initially thinner disk were very similar; the orbit decayed at almost exactly the same rate and the final thickness was only marginally less. A thicker disk was less robust, however; the satellite orbit decayed slightly more quickly and the final disk thickness was substantially greater than in the end state of the standard run. Experiments with other satellite masses did not reveal any surprises.

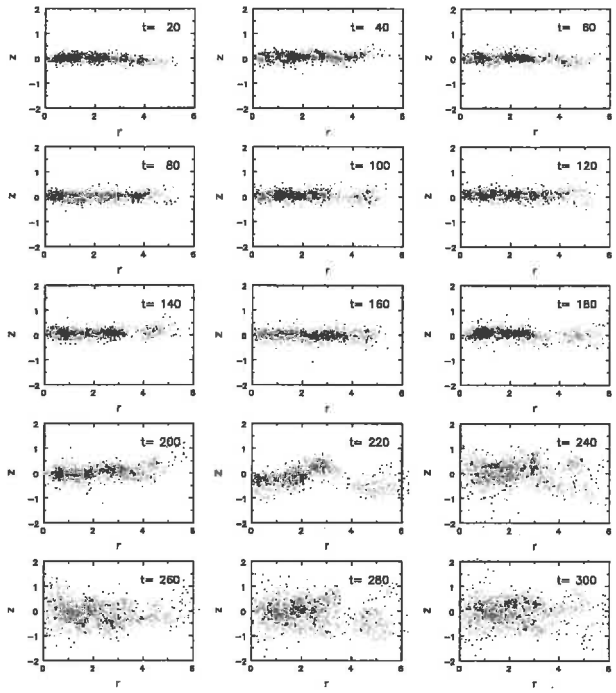

Fig. 4.— Meridional projections of 1500 representative disk particles at equally spaced times. The satellite has passed through the disk three times by $t = 180$ yet the disk has suffered little damage. After $t = 200$, however, the disk convulses dramatically and quickly thickens.

4.2. Interpretation

We are now in a position to interpret these results in terms of the physical processes described in §2. The satellite velocity during the first disk passage is $v \sim 1$, so a star at the center feels perturbations with frequencies up to $\omega \sim v/r_c = 8$. This exceeds $\kappa_z = 1.3$ at $R = 0$ (Figure 2), so the heating is direct, but little heating occurs during these fast passages because the net energy transfer $\Delta E \propto v^{-2}$. At late stages, when the satellite has nearly settled into the disk, it oscillates in z with a frequency ~ 0.6 which is less than $\kappa_z(0)$; therefore there is little or no direct heating, but the satellite can excite bending waves.

The energy input into bending waves is indicated by the difference between the dotted and solid curves in Figure 3d. Whenever the total energy in vertical motion is larger than the energy in random vertical motion, the difference is approximately the energy in bending waves. Increases in random vertical motion generally lag the total vertical energy, perhaps by ~ 10 time units, suggesting that the waves damp sometime after they are excited. This delay is consistent with the propagation time across the disk as given by a typical group velocity (equation 3).

Figure 5a shows the power spectrum of the perturbing force experienced by a particle at the disk center, evaluated from the data shown Figure 3c. The strong peak at $\omega \simeq 0.6$ arises mainly from oscillations of the satellite at late times $t > 240$. There is little power at $\omega \gtrsim \kappa_z(0) \simeq 1.3$, which again shows why direct heating is inefficient. There is significant power at intermediate frequencies $\omega \gtrsim \nu_h \simeq 0.3$, which excites bending waves. The excitation of bending waves mostly occurs at late times when the satellite orbital frequency resonates with the long-wavelength disk modes. To illustrate this, in Figure 5b we have plotted the power spectrum that would arise if the

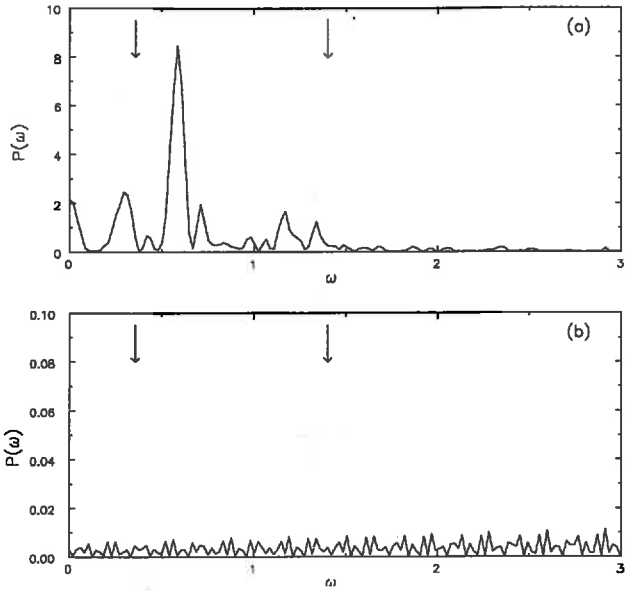

Fig. 5.— (a) The power spectrum of the vertical force shown in Figure 3c; (b) the power spectrum if the force in 3c is multiplied by a window which is unity for $t < 150$ and decays smoothly to zero (as $\cos^2$) between $t = 150$ and $t = 200$. The vertical arrows at $\omega \simeq 0.35$ and 1.3 denote the central values of ν_h and κ_z respectively.

force in Figure 3c were multiplied by a window that is unity at early times and decays smoothly to 0 between $t = 150 - 200$; the strong low-frequency power is removed. Note that the scales in the two panels differ by a factor of 100.

To confirm that most of the heating occurs at late times we have conducted an experiment identical to the standard run up until time 150; we then gradually "vaporized" the satellite (with a $\cos^2$ time dependence) from its initial 5% of the galaxy mass down to that of all the other particles. The results are shown in Figure 6. Even though the satellite passed through the disk twice when it had its full mass and a third time with about half its initial mass, the increase in the vertical random kinetic energy of the disk particles is barely detectable. This result is consistent with the conclusion of Huang & Carlberg (1997) that a satellite does not heat the disk at all if it is tidally disrupted before it reaches the vicinity of the disk.

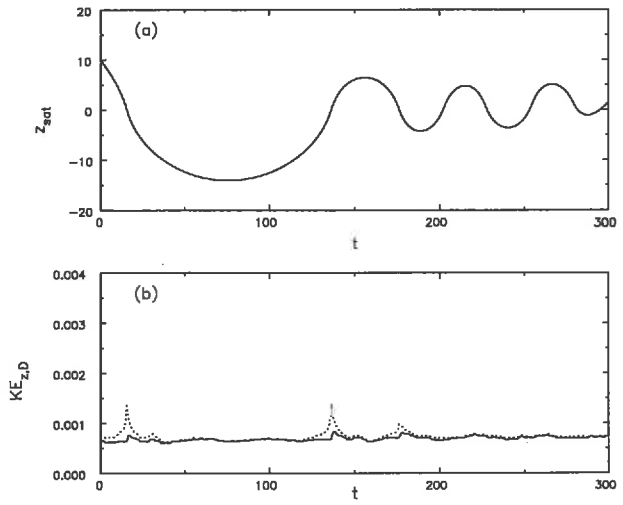

Fig. 6.— As for Figure 3a and 3d, but for an experiment in which the satellite was "vaporized" over the time interval $150 \leq t \leq 200$. The vertical heating of the disk is barely detectable in this case. The residual particle experiences no friction after $t = 200$ because of its negligible mass. The lower panel also demonstrates that an unperturbed disk does not thicken over the course of an experiment.

5. Additional numerical experiments

5.1. Off-center encounters

We are unable to study off-center impacts properly with an axisymmetric $N-$body code. Nevertheless, we may consider the interaction of a massive ring-like satellite with the galaxy – an admittedly artificial arrangement, but one which is still instructive.

The "satellite" in these experiments is a massive ring having 5% of the galaxy mass. The ring initially has no radial or vertical velocity ($v_z = v_R = 0$), but v_ϕ is set so that the ring has sufficient angular momentum to balance the gravitational attraction towards the symmetry axis. The ring mass is added to the calculation grid so that the mutual forces between the satellite and the particles can be calculated using the grid. Because there are no tangential forces in our experiments, the satellite cannot lose angular momentum, but it can give up energy from its vertical motion to the lighter particles of the disk and halo.

We initially performed these ring experiments using the same disk and halo described in §3. In this case we found the satellite did little heating at all. For

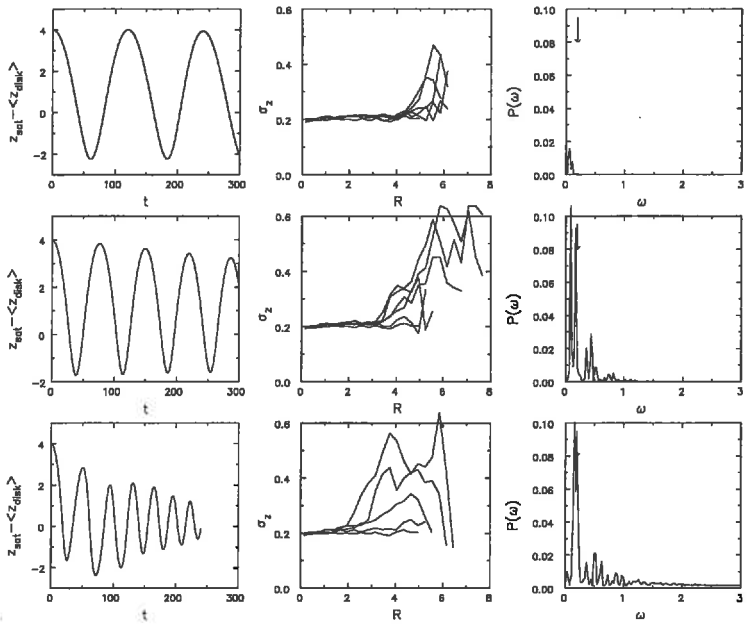

Fig. 7.— Three experiments with ring-like satellites showing the vertical motion of the satellite on the left. The different curves in each center panel show the rms disk thickness as a function of radius at intervals of 60 time units. The power spectrum of the force experienced by a particle at $(R, z) = (4, 0)$ is shown on the right. The satellite started at $z = 4$ in each case and at $R = 8$ (top row), $R = 6$ (middle row) and $R = 4$ (bottom row).

this disk, with thickness $0.1a$, the vertical forcing has little power above the stellar vertical frequencies, κ_z (see figures 2 and 5). Consequently, we use a flabbier disk with double the thickness for these experiments. Figure 7 shows results from three simulations in which the perturber was started at $(R, z) = (8, 4)$, $(6, 4)$ and $(4, 4)$. Recall that the disk edge is at $R = 5$ and the halo mass density is very low beyond this radius.

The satellite started outside the galaxy with $R = 8$ oscillates about the mid-plane with hardly any decay and little energy is transferred to the disk. The satellite started at $R = 6$ decays slowly while the disk begins to thicken near the outer edge only. Finally, the orbit of the satellite started at $R = 4$, which passes through the disk, decays more quickly and disk thickening gradually extends inwards as the orbital period drops. In the top panel, the satellite is well outside the truncation radii of both the disk and the halo and it moves so slowly that the particles can respond adiabatically. As the forcing frequency rises, the perturbation approaches resonance with some particles and the satellite loses energy.

Figure 7 shows that disk particles that are close to resonance absorb energy from the perturber, but it should be noted that most of the energy lost by the satellite is absorbed by the halo particles.

5.2. Forced response of a disk galaxy

In this subsection we consider the response of a disk galaxy to a periodic forced oscillation – in this case, a satellite is driven up and down the rotation axis at a fixed frequency. Although highly unrealistic, this experiment illustrates the importance that vertical resonances play in heating of the disk.

The mass of the perturber in these experiments is $0.01M$ and it is forced to move as

$$z(t) = 0.05a \sin\left(\frac{2\pi t}{\tau}\right), \tag{8}$$

with τ being the oscillation period. The perturbing mass starts in the mid-plane at $t = 0$ and the negative of its initial momentum is shared equally among all the particles of the galaxy. Figure 8 shows the result from an experiment with $\tau = 20$ in our time units. The gravitational coupling between the forced perturber and the surrounding disk is strong enough that the disk center is locked to it; the perturber therefore launches an axisymmetric bending wave that travels radially outwards through the disk. The upward slope of the crests in the left-hand panel shows that the driven bending wave propagates outwards, as expected for WKB bending waves described by equations (2) and (3). The amplitude increases with radius for some distance, as conservation of wave action demands, but then drops again just after the point where localized thickening of the disk occurs, as shown in the right-hand panel.

As described in §2, bending waves are strongly damped at vertical resonances where the wave frequency is nearly equal to the vertical oscillation frequency of disk particles (equation 6). The epicyclic frequency, κ_z, for small-amplitude oscillations is plotted for this model in Figure 2. The forcing frequency is equal to κ_z at $R = 3.43$. This is somewhat outside the radius where maximum disk thickening occurs, $R \simeq 2.5 - 3.0$. This asymmetry is expected for outward propagating waves, since equation (6) shows that significant damping will occur when the vertical frequency is within a few times $k\sigma$ of ω.

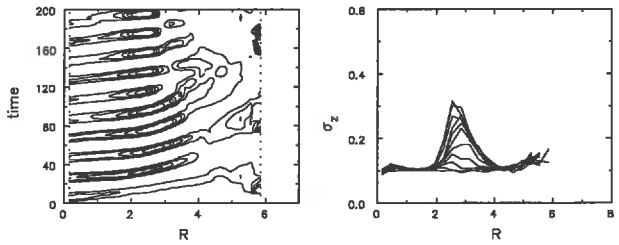

Fig. 8.— An experiment with a forced perturbation at period $\tau = 20$ time units. On the left we contour the mean z displacement of the disk particles as functions of radius and time; the contours show only positive displacements. The different curves in each right hand panel show the rms disk thickness as a function of radius at intervals of 20 time units.

This simulation suggests that disks are heated when a perturber excites bending waves that travel across the disk until their energy is absorbed at the location near to the 1:1 particle resonance.

5.3. Bowl modes

We have attempted to reproduce the axisymmetric "bowl mode" predicted by Sparke (1995) for cold, razor-thin disks inside rigid halos, but without success. These modes are expected to be damped when the halo can respond (Nelson & Tremaine 1996), but in realistic disks they are, in fact, damped much more effectively by the disk stars.

In experiments in which we held the halo rigid, we found that a radially warm and thick disk no longer supports this mode because its frequency, which is set largely by the halo, is usually in resonance with the vertical motion of the particles somewhere in the disk. Initial bends having the shapes of the mode predicted by Sparke decay rapidly causing localized heating even when the halo mass is held rigid. The decay rate was very similar when we substituted a live halo, indicating that all the significant damping occurred in the disk.

5.4. Some puzzles

We have extended the series of experiments with live halos from §5.2 to other forcing frequencies. At most of the forcing frequencies we used we obtained a response not only at the driven frequency but also at a second, well-defined frequency.

When the forcing frequency was high enough for the waves to be Landau damped by the disk particles, we generally obtained two heating peaks, whereas only one was expected. The result shown in Figure 8 is actually quite exceptional. Whenever a second peak occurred, Fourier analysis of the displacements of the disk over time always revealed a second frequency with a resonance where the heating was observed. The extra response frequency was neither a simple multiple nor fraction of the driven frequency. Moving the driving disturbance to a different radius did not change the extra response frequency, nor did changes to its amplitude. In some cases, the heating caused by the extra response exceeded that caused by the driven wave.

At still lower frequencies, for which no 1:1 resonances were present in the disk, we again obtained two responses. With a forcing period $\tau = 80$, for which the 1:1 resonance is right at the disk edge, we were surprised to find that the displacement of the entire disk instantly began to behave as the superposition of two neutral, large-scale bending waves of similar amplitude. The two waves have different frequencies giving rise to beats. We have estimated the two waves to have frequencies 0.077 and 0.068 with negligible growth/decay rates; the higher is the forcing frequency but the lower appears to be a natural oscillation frequency of the whole disk-halo system. We found that the system abruptly stops oscillating as soon as the forcing is turned off. At even lower forcing frequency, $\tau = 120$, the disk-halo "mode" seemed to damp quite quickly, leaving the system to oscillate steadily at the driven frequency.

We have no explanation for these extra frequencies, but believe they are not numerical artifacts since we could reproduce them with other codes. The referee, J Goodman, suggested that they could result from non-linear coupling to an axisymmetric density wave, but we were unable to find any evidence for density waves with appropriate frequencies. We consider this strange behavior to be irrelevant to the conclusions of this paper, since we have seen it only in the artificial circumstances of harmonic external driving.

6. Discussion and conclusions

The goal of this paper has been to gain physical insight into disk heating and thickening caused by the accretion of small satellite galaxies. We have chosen to explore an axisymmetric system in order to isolate the vertical heating phenomenon. This strategy has

the advantage that our simulations are inexpensive, allowing us to sample a broader region of parameter space while avoiding internal evolution and artificial heating from numerical relaxation. We believe that most of the conclusions below also apply to the general case of off-axis satellite accretion.

We have found that the satellite loses little energy to direct heating of disk stars, because most of the power in the satellite force is at frequencies lower than the natural oscillation frequencies of the disk stars. There is substantial heating at late stages, however, through the intermediate process of exciting disk bending waves. Once excited, these waves eventually damp efficiently at wave-particle resonances, thereby heating the disk non-locally. The only significant radial heating also occurs at the time the disk is thickened by the bending waves. Thus, satellites which are tidally disrupted before they are able to excite bending waves do not thicken the disk.

Bending waves can damp by several mechanisms, including dynamical friction from the halo, nonlinear damping at the disk edge, and internal wave-particle resonances. In most cases wave-particle resonance (Landau damping) is by far the strongest damping mechanism; since this mechanism depends strongly on the disk thickness and vertical frequencies, numerical simulations must accurately reproduce these quantities in order to represent the behavior of real galaxy disks.

Thus collective effects can significantly reduce the vertical energy deposited by the satellite only through tilting the disk in an off-axis encounter, as shown by Huang & Carlberg (1997; see also Athanassoula 1996). Tilting the target galaxy, reduces the vertical energy of the satellite about the new disk plane.

We have not explored many important issues discussed by TO and others; for example, we have not simulated the full range of satellite impacts with arbitrary orbital orientations and satellite masses, and we have not attempted to estimate the average heating rate. Since off-center encounters can excite disturbances with $m \neq 0$, which also contribute to heating the disk, we cannot address the actual extent to which disk heating is important in real galaxies.

Many effects that we have ignored, however, such as tidal stripping of the satellite, late star formation, and tilting the disk, tend to make the satellite less destructive. Thus, the heating we obtain is an upper limit that should result from an axial encounter with a low-mass satellite.

This work was supported by NSF grants AST 93/18617 and AST 96/17088 and NASA Theory grant NAG 5-2803 to JAS and was begun during a long visit by JAS to CITA, whose hospitality is gratefully acknowledged. We thank Alar Toomre for many discussions and much advice over an extended period and Jeremy Goodman for a thoughtful referee report.

REFERENCES

Araki, S. 1985, PhD Thesis, MIT

Athanassoula, E. 1996, in *Barred Galaxies and Circumnuclear Activity*, eds. Aa. Sandquist & P. O. Lindblad, Nobel Symposium **98** Lecture Notes in Physics, Volume **474** (Berlin: Springer-Verlag)

Binney, J. & Tremaine, S. 1987, *Galactic Dynamics* (Princeton: Princeton University Press)

Camm, G. L. 1950, MNRAS, 110, 305

Carlberg, R. G. 1987, ApJ, 322, 59

Dubinski, J. & Kuijken, K. 1995, ApJ, 378, 496

Huang, S. & Carlberg, R. G. 1997, ApJ, 480, 503

Hunter, C. & Toomre, A. 1969, ApJ, 155, 747

Lin, D. N. C. & Tremaine, S. 1983, ApJ, 264, 364

Lynds, R. & Toomre, A. 1976, ApJ, 209, 382

Nelson, R. W. & Tremaine, S. 1996, MNRAS, 275, 897

Pfenniger, D. 1991, in *Dynamics of Disc Galaxies*, ed. B. Sundelius, (Gothenburg: Göteborgs University) p. 191

Quinn, P. & Goodman, J. 1986, ApJ, **309**, 472

Quinn, P. J., Hernquist, L. & Fullagar, D. P. 1993, ApJ, **403**, 74

Sellwood, J. A. 1996, ApJ, 473, 733

Sellwood, J. A. & Valluri, M. 1997, MNRAS, 287, 124

Sparke, L. S. 1995, ApJ, 439, 42

Sparke, L. S. & Casertano, S. 1988, MNRAS, 234, 873

Spitzer, L. 1942, ApJ, 95, 329

Spitzer, L. 1958, ApJ, 127, 17

Toomre, A. 1964, ApJ, 139, 1217

Toomre, A. 1966, in *Geophysical Fluid Dynamics*, notes on the 1966 Summer Study Program at the Woods Hole Oceanographic Institution, ref. no. 66-46, p 111

ERROR: typecheck
OFFENDING COMMAND: token

STACK:

-savelevel-
-savelevel-

Disordered Systems and Quantum Chaos (July to December 1997)

Report from the Organisers: JP Keating (Bristol); DE Khmelnitskii (Cambridge); IV Lerner (Birmingham); P Sarnak (Princeton)

Scientific Background and Objectives

The motion of a particle in a random potential in two or more dimensions is chaotic, and the trajectories in deterministically chaotic systems are effectively random. It is therefore no surprise that there are links between the quantum properties of disordered systems and those of simple chaotic systems. The question is, how deep do the connections go? And to what extent do the mathematical techniques designed to understand one problem lead to new insights into the other?

The quantum properties of disordered systems have been the focus of considerable attention in many branches of physics, most notably nuclear physics and condensed matter physics. In the last few years, advances in the field of microelectronics have shifted the focus in condensed matter physics to the study of mesoscopic systems, such as electronic devices that are large on the atomic scale but sufficiently small for quantum coherence effects to be important. In some circumstances the behaviour of these devices is governed by the fact that they have randomly distributed impurities; that is, they are disordered.

The canonical problem in the theory of disordered mesoscopic systems is that of a particle moving in a random array of scatterers. The aim is to calculate the statistical properties of, for example, the quantum energy levels, wavefunctions, and conductance fluctuations by averaging over different arrays; that is, by averaging over an ensemble of different realizations of the random potential. In some regimes, corresponding to energy scales that are large compared to the mean level spacing, this can be done using diagrammatic perturbation theory. In others, where the discreteness of the quantum spectrum becomes important, such an approach fails. A more powerful method, developed by Efetov, involves representing correlation functions in terms of a supersymmetric nonlinear σ model. This applies over a wider range of energy scales, covering both the perturbative and non-perturbative regimes.

In quantum chaos, the goal is to understand the semiclassical asymptotics of the quantum properties of individual classically chaotic systems, examples of which include simple atoms (eg helium), molecules, and also mesoscopic quantum devices. In this case the main tool is Gutzwiller's

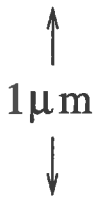

Toomre, A. 1983, unpublished notes

Toomre, A. 1995, unpublished notes

Tóth, G. & Ostriker, J. P. 1992, ApJ, 389, 5

Walker, I. R., Mihos, J. C. & Hernquist, L. 1996, ApJ, 460, 121

Weinberg, M. D. 1986, ApJ, 300, 93

Weinberg, M. D. 1991, ApJ, 373, 391

This 2-column preprint was prepared with the AAS LaTeX macros v4.0.

Recent Newton Institute Preprints

NI97021-NQF **JM Figueroa-O'Farrill, C Köhl and B Spence**
Supersymmmetry and the cohomology of (hyper) Kähler manifolds
hep-th/9705161; Nucl.Phys. B 503 (1997) 614-626

NI97022-NQF **JP Gauntlett**
Duality and supersymmetric monopoles
hep-th/9705025; Nucl.Phys.Proc.Suppl. 61A (1998) 137-148

NI97023-NQF **JP Gauntlett**
Intersecting branes
hep-th/9705011

NI97024-RAG **J Rickard**
Triangulated categories in the modular representation theory of finite groups

NI97025-NQF **P van Baal**
Intermediate volumes and the role of instantons

NI97026-NQF **CJ Houghton, NS Manton and PM Sutcliffe**
Rational maps, monopoles and skyrmions
hep-th/9705151; Nuclear Physics B510 [PM] (1998) 507-537

NI97027-NQF **PS Howe, E Sezgin and PC West**
Aspects of superembeddings
hep-th/9705903

NI97028-NQF **CM Hull**
Gravitational duality, branes and charges
hep-th/9705162; Nucl.Phys. B509 (1998) 216-251

NI97029-NQF **M Abou Zeid and CM Hull**
Instrinsic geometry of D-branes
hep-th/9704021; Phys.Lett. B404 (1997) 264-270

NI97030-NQF **CP Bachas, MR Douglas and MB Green**
Anomalous creation of branes
hep-th/9705074

NI97031-RAG **M Broué, G Malle and J Michel**
Complex reflection groups, braid groups, Hecke algebras

NI97032-NQF **D Zwanziger**
Renormalization in the Coulomb gauge and order parameter for confinement in QCD

NI97033-NQF **E Shuryak and A Zhitnisky**
The gluon/charm content of the $\eta\prime$ meson and instantons
hep-ph/9706316; Phys.Rev. D57 (1998) 2001-2004

NI97035-RAG **K Magaard and G Malle**
Irreducibility of alternating and symmetric squares
Manuscripta Mathematica 95, 169-180 (1998)

NI97036-STA **N Linden and S Popescu**
On multi-particle entanglement

NI97037-NNM **M Studený and RR Bouckaert**
On chain graph models for description of conditional independence structures

NI97038-RAG **M Geck and G Malle**
On special pieces in the unipotent variety

NI97039-NNM **SP Luttrell**
A unified theory of density models and auto-encoders
DERA report DERA/CIS/CIS5/651/FUN/STIT/5-4 31 October 1997

NI97040-NNM **CKI Williams and D Barber**
Bayesian classification with Gaussian processes

NI97041-NNM **TS Richardson**
Chain graphs and symmetric associations
Learning in Graphical Models, MIT Press Jan 98 M Jordan (ed.)

NI97042-NNM **A Roverato and J Whittaker**
An importance sampler for graphical Gaussian model inference

NI97043-DQC **MR Haggerty, JB Delos, N Spellmeyer et al**
Extracting classical trajectories from atomic spectra

NI97044-DQC **S Zelditch**
Level spacings for quantum maps in genus zero

NI97045-DQC **U Smilansky**
Semiclassical quantization of maps and spectral correlations

NI97046-DQC **IY Goldscheid and BA Khoruzhenko**
Distribution of Eigenvalues in non-Hermitian Anderson models
Phys. Rev. Lett. 80 (1998) No.13, 2897-2900

NI97047-DQC **G Casati, G Maspero and DL Shepelyansky**
Quantum fractal Eigenstates

NI98001-STA **N Linden and S Popescu**
Non-local properties of multi-particle density matrices

NI98002-AMG **J-L Colliot-Thélène**
Un principe local-global pour les zéro-cycles sur les surfaces fibrés en coniques au-dessus d'une courbe de genre quelconque

NI98003-AMG **RGE Pinch and HPF Swinnerton-Dyer**
Arithmetic of diagonal quartic surfaces, II

NI98004-AMG **DR Heath-Brown**
The solubility of diagonal cubic diophantine equations

NI98005-AMG **B Poonen and M Stoll**
The Cassels-Tate pairing on polarized Abelian varieties

NI98006-AMG **R Parimala and V Suresh**
Isotropy of quadratic forms over function fields of curves over p-adic fields

NI98007-AMG **E Peyre**
Application of motivic complexes to negligible classes

NI98008-AMG **E Peyre**
Torseurs universels et méthode du cercle

NI98009-RAG **JA Green**
Discrete series characters for $GL(n, q)$

NI98010-DQC **K Zyczkowski, P Horodecki, A Sanpera et al**
On the volume of the set of mixed entangled states

NI98011-DQC **K Zyczkowski and W Slomczyński**
Monge distance between quantum states

NI98012-DAD **JA Sellwood, RW Nelson and S Tremaine**
Resonant thickening of disks by small satellite galaxies